JOURNAL OF MATERIALS SCIENCE 33 (1998) 4357–4364

Hydrothermal degradation of chemical vapour deposited SiC fibres

T. KRAFT, K. G. NICKEL
Institut für Mineralogie, Petrologie und Geochemie, Universität Tübingen, Wilhelmstraße 56, D-72074 Tübingen, Germany

Y. G. GOGOTSI
Department of Mechanical Engineering, University of Illinois at Chicago, 842 West Taylor Street, Chicago, IL 60607, USA
E-mail: ygogotsi@uic.edu

The interaction of chemical vapour-deposited (CVD) SiC fibres with H_2O at 200 MPa and 400–700 °C (673–973 K), was investigated. With increasing temperature and time, the smooth surface of the amorphous SiC fibre becomes rough and sponge-like. This modification can be controlled by adjusting temperature and duration of the hydrothermal treatment. CVD SiC dissolves in supercritical water in a first order reaction with $E_a = 150$ kJ mol^{-1}. According to thermodynamic calculations, the main products are SiO_2, CH_4 and H_2. The formation of carbon is also predicted. Films of amorphous and graphitic carbon have been observed, but only small areas of the fibres were coated with carbon. Amorphous silica, quartz, cristobalite and keatite were deposited on the surface of fibres in larger quantities

1. Introduction

Silicon carbide (SiC) fibres are commonly used as reinforcement components in ceramic and metallic matrices [1]. Two kinds of fibres are commercially available: (1) thick chemical vapour-deposited (CVD) SiC fibres made by thermal decomposition of volatile methyl chloride silanes on hot carbon or tungsten monofilament substrates [2]; (2) thin SiC fibres such as Nicalon® [3] or Tyranno® [4] fibres which are obtained by pyrolysis of polymeric organometallic precursors such as polysilanes and carbosilanes.

For use in hot-water-containing environments, the hydrothermal corrosion of SiC powder, Tyranno fibres, and SiC ceramics has been investigated in detail [5–9]. In both cases, the formation of carbon with variable structures between graphitic sp^2- and diamond-like sp^3-carbon has been observed on the SiC surface [10–14]. It is believed that the carbon rather forms by extraction of silicon out of the carbide than by deposition out of the fluid. This feature may be important for simple and tailored carbon coatings on SiC which may act as an interphase between SiC and matrix in composites to improve the fracture toughness and maximize the work of fracture in such materials [15].

In this paper we report our investigations on hydrothermal corrosion of CVD SiC fibres in distilled water at 200 MPa with particular attention to corrosion kinetics and carbon formation.

2. Experimental procedure

CVD SiC filaments, manufactured by Textron Specialty Materials, Lowell, MA with a diameter of 131.3(6) μm were used. Approximately 50 μm amorphous SiC (Fig. 1c) was deposited on a low-cost carbon monofilament substrate of about 30 μm diameter. The CVD Sic was connected to the carbon monofilaments through a SiC/carbon interlayer of about 1 μm thickness. The fibres were cut into pieces less than 1.5 cm in length. They were placed with distilled water into gold capsules, 3 mm diameter and 2.5 cm length. The capsules were welded to prevent the exchange of material during the experiment. Typically, a capsule contained five fibres (2–2.5 mg) with an eight-fold amount of water (16–20 mg). The capsules were placed in tube-type pressure vessels made of René 41 superalloy [16] and heated to temperatures between 400 and 700 °C under a hydrostatic pressure of 200 MPa. From those fibres which were covered with silica after the experiments, two from each capsule were leached in 38% hydrofluoric acid to remove the silica.

The fibres and other reaction products where analysed by scanning electron microscopy (SEM) and micro-Raman spectroscopy using a Dilor Labram micro-Raman spectrometer with a charge coupled device (CCD) detector. Excitation was accomplished by using helium/neon and argon ion-lasers operating at wavelengths of 628.8 and 514.5 nm, respectively.

The recession of the SiC surface was measured through the decrease in the fibre diameter. Half the

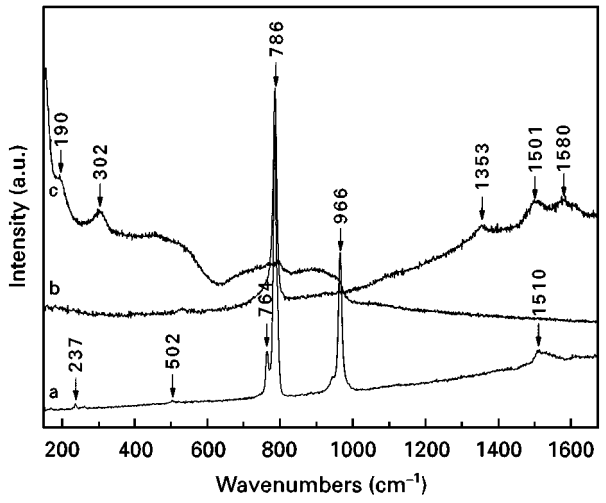

Figure 1 Raman spectra of SiC, excitation wavelength = 632.8 nm. (a) α-SiC powder, (b) β-SiC powder, (c) amorphous CVD SiC.

decrease of the diameter is the linear recession of the SiC surface. The diameters of the fibres were measured using an Olympus BH-2 microscope equipped with a CCD-camera and Lucia® image processing tools. For each experiment, four different fibres were measured in three to seven different cross-sections. The diameters were taken exclusively from spots not covered by silica scales. If necessary, the silica was removed mechanically or by HF-leaching. However, no significant differences in the diameters within fibres from one experiment with different post treatments have been observed. The accuracy of the values obtained is better than 1 μm.

3. Results

All valid experiments and their results are listed in Table I.

3.1. Morphology of the CVD SiC surface after hydrothermal treatment

Depending on temperature and exposure time, noticeable changes in the surface structure of the CVD SiC are observed by scanning electron microscopy (SEM). Already after 4 h at 400 °C, the smooth, only slightly structured surface of pristine CVD SiC (Fig. 2a) is considerably roughened (Fig. 2b). Roughness of the surface increases with increasing exposure time (Fig. 2c) and particularly with increasing temperature. A considerable degradation of the fibres starts at 500 °C. A similar behaviour was observed for SiC powders [17]. Thus, after 32 h at 600 °C, the fibre surface is covered with small pits (Fig. 2d) which grew larger after 16 h at 650 °C (Fig. 2e) while a sponge-like residue was found after 4 h at 700 °C (Fig. 2f).

After an initial period, the structure of the surface depends only on the temperature, while the exposure time accounts for the degree of degradation. Usually, a homogeneous surface remains. Only in a few cases, e.g. after 32 h at 600 °C, inhomogeneous surface structures are observed (Fig. 3). Etching with hydrofluoric acid removes silica from the CVD SiC surface but does not alter the surface significantly. Comparing the HF etched surface with the surface after mechanical removal of silica scales showed only a very slight smoothing (128 h at 500 °C) or etching (600 °C, 32 h).

Experiments in larger volumes (open capsules) or in temperature gradients allow for complete dissolution of silica or its precipitation off the fibres. In such cases, HF etching was no longer necessary. Thus, a specific and selective modification of the surface of the CVD SiC fibres can be accomplished by hydrothermal processing.

3.2. Kinetics of the CVD SiC degradation

The degradation of the CVD SiC fibres has been studied in the temperature range between 500 and 700 °C. Depending on the reaction conditions and reaction products, different kinetics can be assumed. The activity of the CVD SiC surface is expected to be constant at one temperature. Thus, the degradation rate depends solely on the local water activity at the CVD SiC surface in a first order reaction. Assuming active corrosion (no formation of protective layers) in an excess of water, linear loss of material is expected. Passive corrosion (formation of protective layers) should result in parabolic kinetics. In all experiments, a large excess of water was present.

Fig. 4 shows the recession of the CVD SiC surface plotted against exposure time. The results for each temperature are best fitted assuming linear degradation. Conclusively, active corrosion without any formation of a protective layer on the fibres must have taken place. The activity of water must have been approximately constant at each reaction at each temperature. The results fit well an Arrhenius plot (Fig. 5). The slope of the plot is -7843 K, which corresponds to an activation energy E_a of 150 kJ mol^{-1}. This is slightly less than 169–194 kJ mol^{-1} reported for a crystalline SiC powder [5].

3.3. Silica formation

Variable silica scales were observed on CVD SiC fibres after hydrothermal experiments. Initially (e.g. after 4 h at 600 °C, Fig. 6a), scales of small silica spheres of approximately 250 nm diameter form on the SiC surface and grow with time. Homogeneous layers of spheres with diameters up to 10 μm have been observed.

In the next stage, thick and brittle silica scales (Fig. 6b and d) cover the fibres. In a few cases single crystals like in Fig. 6c have been observed. Fig. 6d shows that silica scale and the CVD SiC surface under degradation do not intergrow. Owing to poor adhesion, the silica scales could thus be easily mechanically removed from the fibres and parts were often found on the bottom of the capsules. In addition, silica also precipitates on the walls of the gold capsules. Thus it is indicated that the formation of silica layers, scales, or crystals takes place from the fluid through a continuous dissolution/precipitation process.

After an initial period, the dissolution/precipitation process is expected to be in equilibrium during the

TABLE I Experiments on hydrothermal degradation of CVD SiC fibres at 200 MPa

Treatment			Observations		
Temp. (°C)	Time (h)	Recession (μm)	Overall	SEM	Micron-Raman spectroscopy
		Pristine	Black surface (surf.)	Smooth, slightly structured surface (Fig. 2a)	Amorphous (am.) SiC (Fig. 1c)
400	4	0.0	No silica (SiO_2), golden iridescent surface	Slightly rough surface (Fig. 2b)	Am. SiC (Fig. 1c)
400	256	0.3	No SiO_2, black iridecent surface	Roughened fine structured surface (Fig. 2b)	Am. slightly modified SiC
450	64	0.2	Few small SiO_2 grains, matt grey to black surface	Roughened surface with smoothed ground	Am. SiC with traces of am. carbon
450	128	0.6	Some quartz crystals		Am. SiC, traces of am. carbon
450	256	0.3	Matt grey to black iridecent surface with SiO_2 and carbon particles	Fine structured rough surface with particles of 2 μm	Am. SiC, particles: variable graphitic and Am. carbon
500	1	0.1	Few small SiO_2 grains, matt surface	Roughened fine structured surface like Fig. 2c	Am. SiC
500	4	0.2	Black surface with many small SiO_2 crystalites		Am. SiC
500	128	4.1	Thick transparent shell of SiO_2 on bronze iridescent SiC surface	Holocrystalline SiO_2 shell on fine structured rough SiC surface (Fig. 6b and d) HF-etching: slightly smoothed SiC surface	Am. SiO_2 with crystobalite. HF etching: am. SiC with some fatty scales of graphitic carbon like Fig. 9b
500	256	7.3	Capsule with SiO_2 crystals, few SiO_2 crystals and spheres on fibres		Am. SiC, am. SiO_2 and quartz with carbon
550	1	0.1	Black surface, with some few particles, no SiO_2 observed	Fine structured surface roughness in between Fig. 2c and d	Am. SiC, particles out of am. and graphitic carbon
550	4	0.4	Broken fibres with bronze iridescent surface covered with small particles		Am. SiC everywhere with traces of disordered graphitic carbon like Fig. 8b
550	48	3.6	Capsules and fibres with SiO_2 crystals, brownish fibre surface	Roughened surface covered with small spheres like in Fig. 6a	Am. SiC, am. SiO_2, cristobalite und quartz, traces of am. and graphitic carbon like Fig. 9a and b
550	96	7.3	Much SiO_2 in the capsule, fibres only partially covered with SiO_2		Am. SiC surface with particles of SiO_2 and graphitic carbon like Fig. 9b
550	128	19.1	Large crystals (Fig. 6c) in capsule and on fibres, black fibre surface	Rough surface covered with spheres (0.3 μm diameter), HF-etched: rough structured surface carbon scales (Fig. 8)	Quartz and am. SiO_2 HF-etched: partially crystallized SiC, am. and graphitic carbon like Fig. 9a and b
550	192	22.7	Much SiO_2 in capsule, fibres covered with little or no SiO_2		Am. carbon in quartz and am. SiO_2, partially crystallized SiC, variable graphitic carbon, on HF-etched fibres too
600	4	1.2	Bronze iridescent surface with some crystallites	Roughened surface covered with small spheres (Fig. 6a)	Only am. SiC
600	32	10.7	Black fibres with crystals, HF-etched: bronze iridescent fibres	Fine structured rough surface, slightly sharpened by HF-etching (Fig. 2d), in parts covered with spongy SiC (Fig. 3)	Quartz and am. SiO_2 with graphitic carbon, HF-etched: am. SiC and graphitic carbon like Fig. 9b
600	48	12.4	SiO_2 shell cracked off the fibres, brown to black surface		Am. SiC with some scales of graphitic carbon like Fig. 9b, quartz and am. carbon
600	64	24.6	SiO_2 shell partially cracked away, brownish SiC-surface		Cristobalite and am. SiO_2, disordered graphitic carbon, HF-etched: am. SiC and am. carbon like Fig. 9a
650	1	0.8	Brownish surface, no SiO_2 found	Surf. covered with spheres of 1 μm diameter	Am. SiC surface with traces of am. and graphitic carbon
650	4	7.5	Black fibre covered with a thick shell of spherical SiO_2	Big (10 μm) and small (0.4 μm) SiO_2 spheres HF-etched: rough spongy surface like Fig. 2e and f	Am. SiO, HF-etched: am. SiC surf. with am. and graphitic carbon like Fig. 9a and b
650	8	10.0	Capsule filled and fibres covered with a thick shell of spherical SiO_2, HF-etched: black–golden iridescent surface		Am. SiO_2 quartz and cristobalite. HF-etched: am. SiC everywhere covered with traces of carbon, scales of am. and graphitic carbon like Fig. 9a and b
650	16	19.3	SiO_2 shell cracked away, black SiC-surface, HF-etched: iridescent surface	Rough surface with some very small sheres, HF-etched: rough spongy surface (Fig. 2e) with carbon scales like Fig. 8	Am. SiO_2, not etched and HF-etched: partially crystallized SiC and graphitic carbon like Fig. 8b and c
650	24	23.3	All SiO_2 in capsule, none on fibres		Am. SiO_2, partially crystallized SiC, am. and graphitic carbon like Fig. 9a and c
700	5	20.9	Severely corroded fibre in a SiO_2 shell	HF-etched: sponge-like surf. (Fig. 2f)	Am. SiO_2 spheres with carbon, HF-etched: partially crystallized SiC, am. and graphitic carbon like Fig. 9a and c

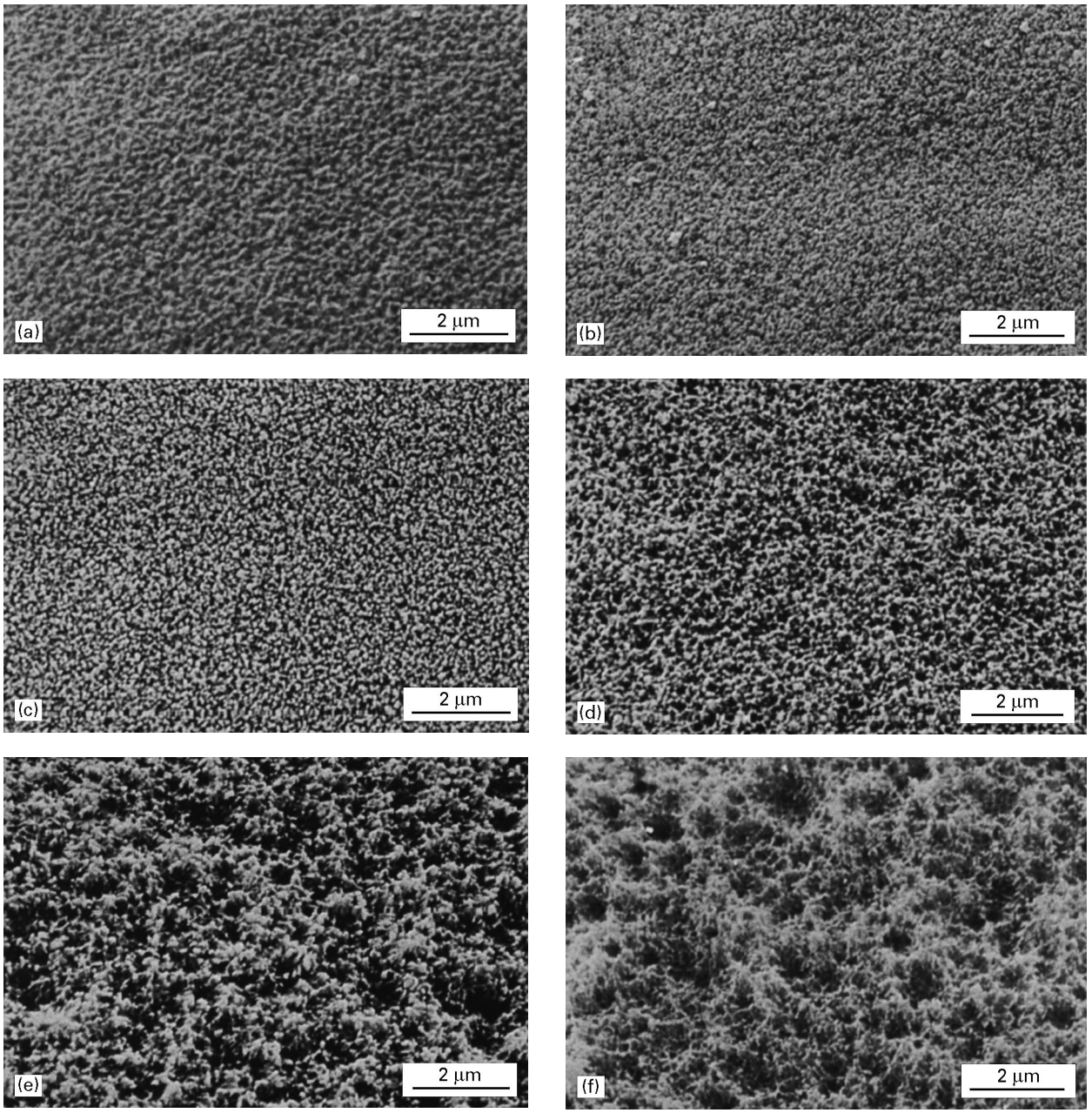

Figure 2 Micrographs of the structure of CVD SiC fibres: (a) as-received; (b) after 4 h at 400 °C; (c) after 256 h at 500 °C; (d) after 32 h at 600 °C, HF etched; (e) After 16 h at 650 °C, HF etched; (f) after 5 h at 700 °C, HF etched.

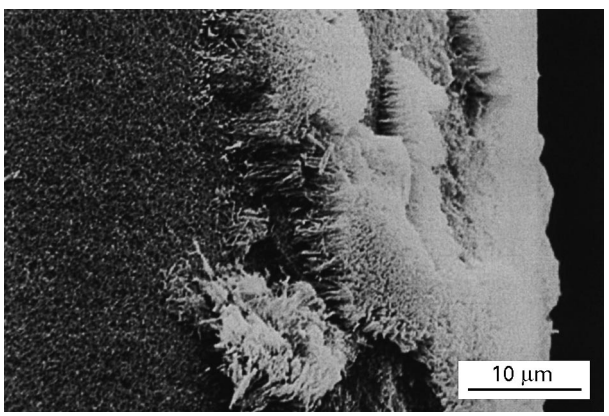

Figure 3 Inhomogeneous CVD SiC surface after 32 h at 600 °C, HF etched.

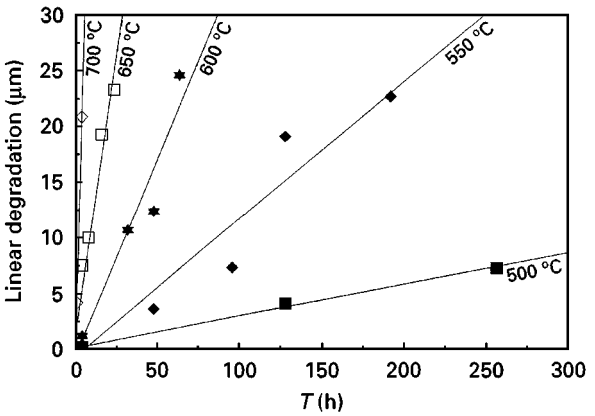

Figure 4 Plot of the time and temperature dependencies of the recession of CVD SiC.

experiment. Under 2 kbar at 700 °C the solubility of SiO_2 in H_2O should always be less than 5 g kg^{-1} [18], which is a maximum of 0.1 mg per capsule. Thus, additional precipitation while quenching and drying the opened capsules at 110 °C may change the surface of the fibres but would not account for thicker scales.

In most cases, optical microscopy and micro-Raman spectroscopy show amorphous opal-like silica, which often contains carbon and water. As the silica scales and crystals always remain colourless, the carbon content must be very small. In many instances, micro-Raman spectroscopy indicates the formation of both quartz and cristobalite. X-ray diffraction of the silica scales showed predominantly quartz with significant amounts of cristobalite and a considerable amount of keatite (Fig. 7).

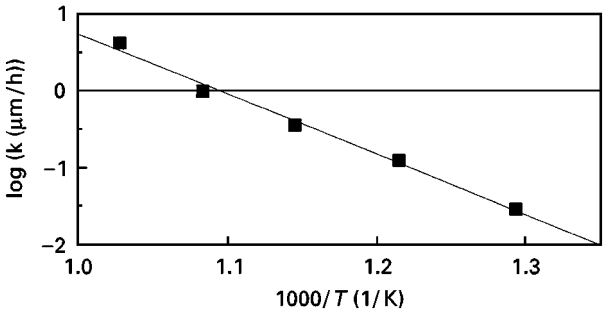

Figure 5 Arrhenius plot of the degradation of CVD SiC.

3.4. Carbon formation

The main objective of the present investigation was to study the possibility of the carbon coating of SiC under hydrothermal conditions [10–13]. The hydrothermal method has been applied to Tyranno® fibres [12], α-SiC platelets, β-SiC powder, and single crystals [11] and should be extended to CVD SiC fibres.

No free carbon was observed on the surface of as-received fibres (Fig. 1c). The formation of carbon has been observed in all experiments at $T \geqslant 550$ °C and the experiments with $t \geqslant 64$ h and 500 °C and $t \geqslant 128$ h at 450 °C. However, a homogeneous carbon coating of the fibres has not been observed. Only at the experiments conducted at 650 °C, could amorphous carbon [19] be detected everywhere on the spongy surface by micro-Raman spectroscopy. Because no homogeneous carbon coating is seen by SEM, the carbon coating must be of submicrometre thickness.

In some experiments, isolated carbon scales were found (Fig. 8a), but their origin may be different. While some scales seem to be grown out of the CVD-SiC by oxidative extraction of silicon (Fig. 8b), other scales appear to have been deposited from the fluid (Fig. 8c). No dependence of the kind of carbon formed under the experimental conditions and especially the reaction temperatures, has been found. Usually, in one experiment, different kinds of carbon are formed. The structures vary from weakly ordered (Fig. 9c, $L_a \sim 5$ nm [20]) and finely dispersed disordered graphite (Fig. 9b, $L_a \sim 3$ nm [20]) to amorphous carbon (Fig. 9a) [19, 21]. According to the Raman spectra

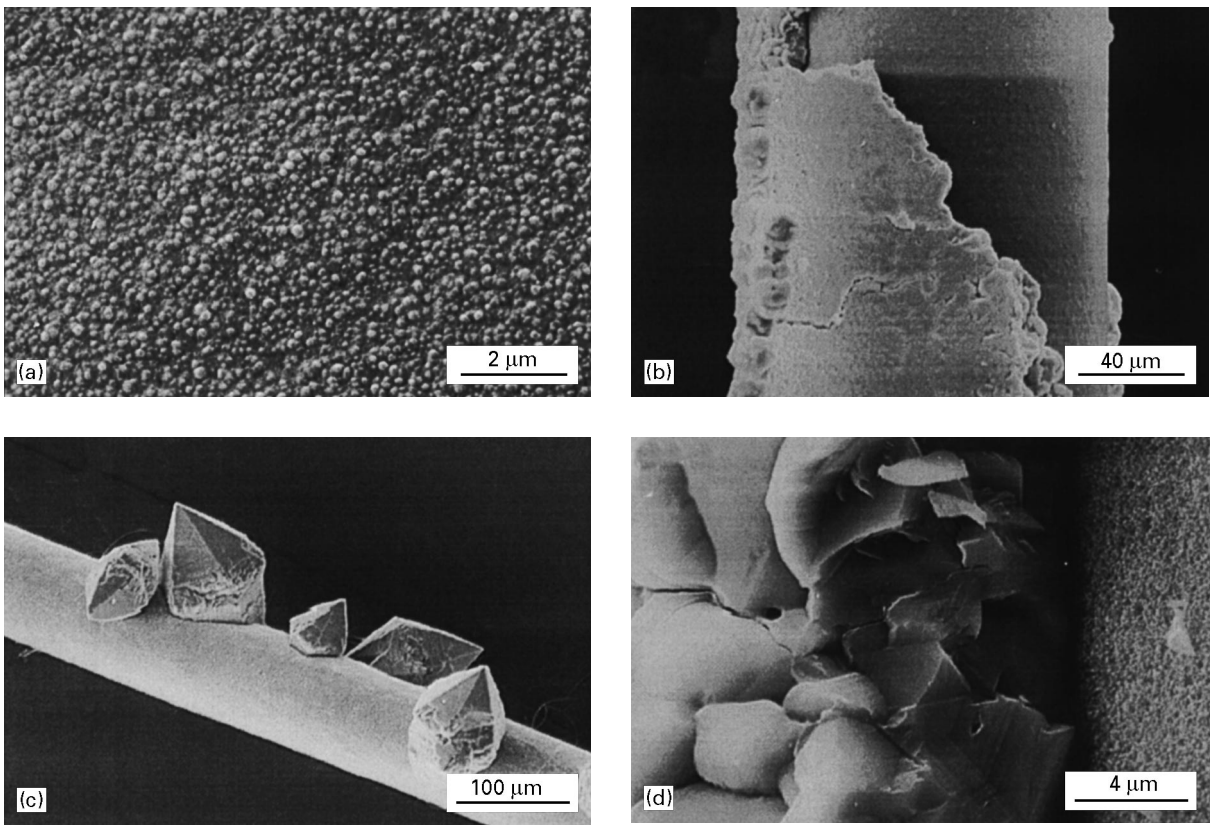

Figure 6 Micrographs of silica scales on CVD SiC fibres. (a) Small spheres after 4 h at 600 °C, (b) Macroscopic scale after 128 h at 500 °C, (c) quartz single crystals after 128 h at 550 °C, (d) Macroscopic scale on the fibre surface after 128 h at 500 °C

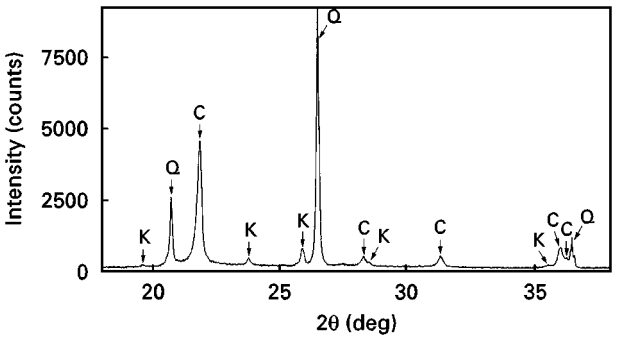

Figure 7 XRD pattern of silica deposites; Q, quartz, C, cristobalite; K, keatite.

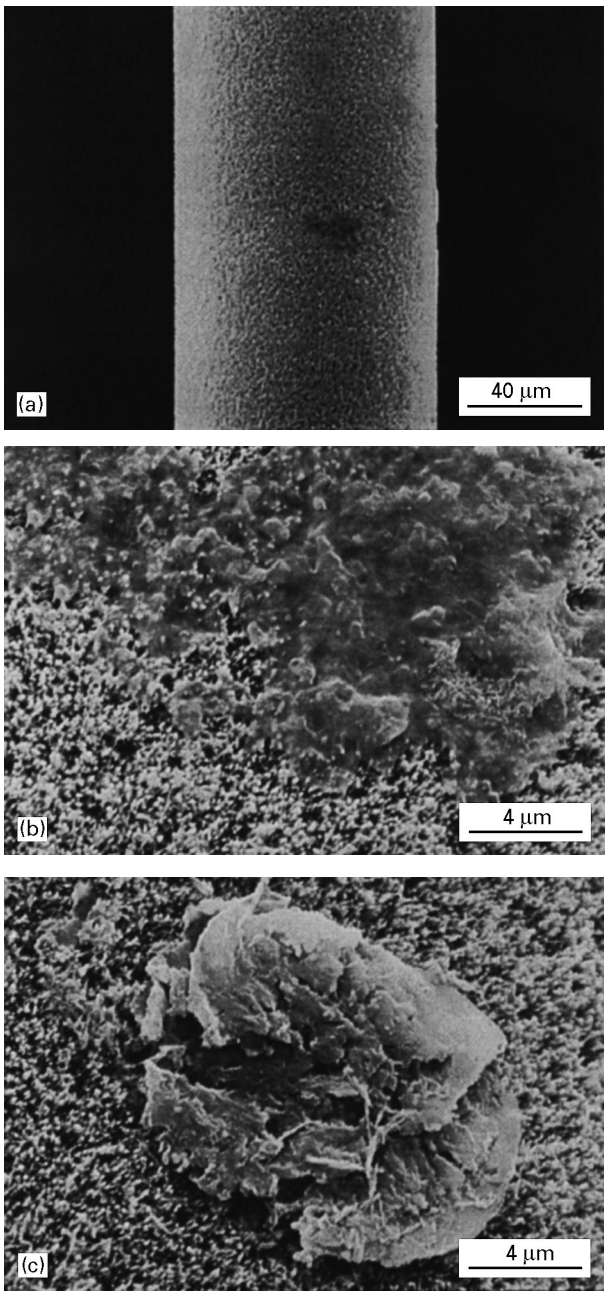

Figure 8 Carbon films on CVD SiC fibre after 128 h at 550 °C, HF etched.

(Fig. 9), predominantly graphitic sp^2-bonded carbon forms as indicated from the broad bands around 1600 and 1330 cm^{-1}. Sp^3-contributions may be present in some carbons as supported from bands at about 1164

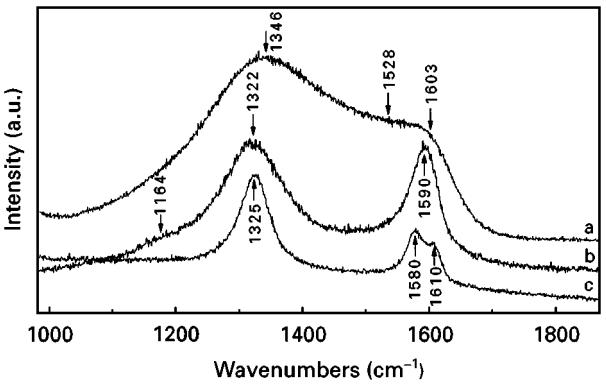

Figure 9 Raman spectra of carbon, excitation wavelength = 623.8 nm. (a) Amorphous carbon, (b, c) nanosized and disordered graphite carbon.

and 1528 cm^{-1} [22, 23] which are unequivocally present after deconvolution of the spectra.

3.5. Thermodynamic calculations

We conducted thermodynamic calculations using Chemsage 3.0 for a pressure of 200 MPa in the temperature range from 300–100 °C. The numerous possible species in the C–H–O system have been constrained to the relevant binary molecules CH_4, CO, CO_2 and H_2O. The calculations are in qualitative agreement with those of Jacobson *et al.* [13]. Fig. 10 shows the activity of the condensed phases in this system, SiO_2 C, and SiC at 500 °C as a function of the amount of water added. This computation is typical for the whole temperature range under investigation: SiO_2 is stable in the whole range. SiC becomes unstable shortly before and carbon becomes unstable shortly after the H_2O:SiC molar ratio of 2:1 is achieved. This corresponds to the reactions

$$SiC + 2H_2O \rightleftharpoons SiO_2 + CH_4 \quad (1)$$

$$SiC + 2H_2O \rightleftharpoons SiO_2 + C + 2H_2 \quad (2)$$

Carbon, methane, and other hydrocarbons can be oxidized by water forming CO, CO_2 and H_2. Fig. 11 shows the temperature-dependent fugacity of the volatile compounds for the H_2O:SiC molar ratio of 1:1. The high relative fugacities of CH_4 and H_2 indicate that both Reactions 1 and 2 take place, but reaction 1 is predominant.

According to these results, complete dissolution of carbon and SiC should occur in the excess of water applied in the experiments. This is apparent at the beginning of the reaction, when all SiO_2 is dissolved. But when the saturation of the fluid with SiO_2 is reached and precipitation of silica occurs, this can result in partially protective layers. The local activity of H_2O is lowered, thus allowing for the formation of carbon. This seems to be not only a local but also a temporary event. Otherwise degradation of the fibres as observed in the change of diameter would be more irregular. Although carbon is thermodynamically unstable under the reaction conditions, it persists because of its low dissolution rates. A

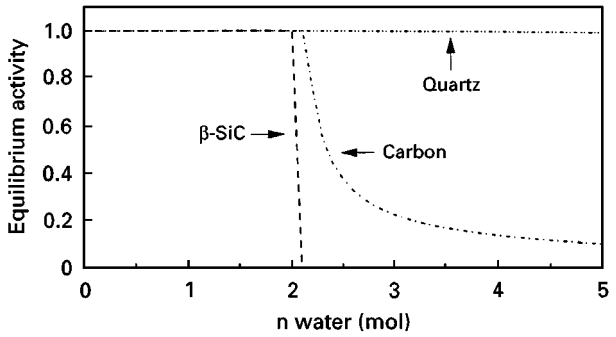

Figure 10 Equilibrium activity of SiC, SiO_2 and carbon for compositions of 1 mol SiC plus variable amounts of H_2O at 500 °C and 200 MPa.

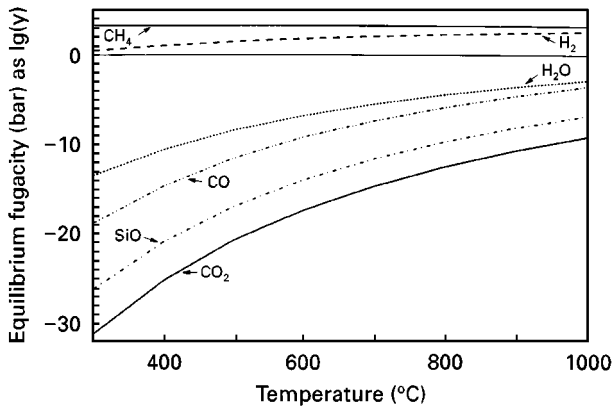

Figure 11 Temperature dependence of the equilibrium fugacity of CH_4, H_2, H_2O, CO, CO_2, and SiO at 200 MPa for a composition of 1 mol SiC plus 1 mol H_2O.

noticeable dissolution of carbon under hydrothermal conditions starts above 700 °C [24].

4. Discussion

Three noteworthy results must be discussed in detail.

1. Formation of carbon on CVD SiC fibres by hydrothermal processing is not as easy to accomplish as on Tyranno® fibres. Structural differences of both amorphous materials may favour or unfavour carbon formation, but differences in the chemical composition may be crucial. In addition to amorphous SiC, TiC, and TiO_2 Tyranno® fibres contain considerable amounts of free carbon [4, 11–13], which will arise the activity of carbon to 1 even in excess H_2O and can act as internal seed for further carbon formation. On the other hand, the amorphous CVD-SiC under investigation does not contain any free carbon (Fig. 1c).

Nonetheless, selective and homogeneous carbon coating of amorphous CVD-SiC by hydrothermal treatment is possible. The hydrothermal reaction conditions must be modified in order to increase the probability of Reaction 2. This can be done by adding "carbon buffers" like organic C–H–O compounds to the fluid and is the subject of a current investigation. Another way for carbon coating of CVD SiC fibres, which may work better in this case, is done by reaction with chlorine-containing gases [25]. On the other hand, this method does not work well in the case of SiC powders and Tyranno® or Nicalon® fibres. Thus, we have access to two different complementary methods of carbon coating by extraction of silicon from SiC [26].

2. The activation energy, E_a, for hydrothermal degradation of CVD SiC is considerably lower than for crystalline SiC powder [5]. This can be ascribed to the structure of the CVD SiC deposited on the carbon monofilament. It is amorphous and not β-SiC powder in Fig. 1. Amorphous substances are thermodynamically and kinetically less stable than the crystalline modifications. This accounts for the fact that E_a is lower and that the corrosion of the CVD SiC on the fibres is faster that the corrosion of α- and β-SiC. The fact that amorphous SiC degrades easier than α- and β-SiC may also be the reason that Reaction 1 becomes even more favoured than Reaction 2 which restrains the formation of carbon.

Even though the data come from experiments with both amorphous and crystalline SiC, a pressure dependency of E_a for hydrothermal degradation of SiC is indicated, with E_a decreasing with increasing pressure. While 194 kJ mol^{-1} was found at 10 MPa, an even lower value of 167 kJ mol^{-1} was found at 100 MPa [5]. We obtained $E_a = 150$ kJ mol^{-1} at 200 MPa.

3. Linear kinetics are encountered for degradation of CVD SiC fibres. This means that the silica scale formed on the fibres is non-protective. This is revealed by Fig. 6d which shows that the silica scale does not adhere to the SiC surface. Thus, water can easily intrude via convection or diffusion through pores, cracks, and grain boundaries in the silica scales into the gap between the silica scale and SiC core. Consumption of water and the formation of methane at the SiC surface is much slower than diffusion and convection of water and methane to and from the SiC core.

In reports on the hydrothermal degradation of SiC powders [5, 6, 27], it has been stated that its kinetics should follow a hyperbolic law best fitted with a Jander-type equation due to protective silica scales. Diffusion of H_2O and CH_4 through the SiO_2-scale should become rate determining. Our data do not confirm the formation of a protective silica scale. Because we did not detect protective behaviour of even very thick and compact silica scales in our experiment on CVD SiC fibres, as well as on other SiC samples, we assume that the silica scale on crystalline SiC powder is not protective.

5. Conclusion

Hydrothermal treatment is a versatile method to modify the surface of CVD SiC fibres. Mainly depending on the reaction temperature, the roughness of the CVD-SiC surface can be varied selectively from plain and smooth over different intermediate stages, to sponge-like. Thus, the surface properties of the CVD-SiC fibres can be tailored in order to control matrix–fibre interaction in composite materials via infiltration of the matrix into the fibres.

In contrast to SiC powders and Tyranno Si(Ti)C(O) or Nicalon SiC fibres from organometallic precursors,

hydrothermal leaching of CVD SiC fibres under the conditions of our experiments did not produce a homogeneous carbon coating. Only very thin (<100 nm) or inhomogeneous carbon films were obtained in our experiments. Moreover, it is possible to supress the formation of carbon by choosing certain reaction conditions.

Acknowledgements

We would like to thank Linus U. J. T. Ogbuji for the supply of the SiC fibres and the Deutsche Forschungsgemeinschaft (grant Ni 299/4) for financial support. Y.G.G. was supported by UIC campus Research Board.

References

1. T. F. COOKE, *J. Am. Ceram. Soc.* **74** (1991) 2959.
2. J. O. CARLSONN in "Encyclopedia of Material Science and Engineering", edited by M. B. Bever (Pergamon Press, Oxford, 1996) p. 4406
3. P. LE COUSTUMER, M. MONTHIOUX and A. OBERLIN, *J. Euro. Ceram. Soc.* **11** (1993) 95.
4. N. M. D. BROWN and H. X. YOU, *J. Mater. Sci.* **28** (1993) 121.
5. M. YOSHIMURA, J. -I. KASE and S. SOMIYA, *J. Mater Res.* **1** (1986) 100.
6. *Idem*, in Proceedings of the Second International Symposium, "Ceramic Materials and Components for Engines", Germany, October 1986, edited by W. Bunk and H. Hausner, p. 529.
7. H. HIRAYAMA, T. KAWAKUBO and A. GOTO, *J. Am. Ceram. Soc.* **72** (1989) 2049.
8. Y. G. GOGOTSI and M. YOSHIMURA *ibid.* **78** (1995) 1439.
9. *Idem*, *J. Mater. Sci. Lett.* **14** (1995) 755.
10. Y. G. GOGOTSI, K. G. NICKEL, D. BAHLOUL-HOURLIER, T. MERLE-MEJEAN, G. E. KHOMENKO and K. P. SKJERLIE, *J. Mater. Chem.* **6** (1996) 595.
11. Y. G. GOGOTSI, P. KOFSTAD, M. YOSHIMURA and K. G. NICKEL, *Diamond Relat. Mater.* **5** (1996) 151
12. Y. G. GOGOTSI and M. YOSHIMURA, *Nature* **267** (1994) 628.
13. N. S. JACOBSON, Y. G. GOGOTSI and M. YOSHIMURA, *J. Mater. Chem.* **5** (1995) 595.
14. R. ROY, D. RAVICHANDRAN, A. BADZIAN and E. BREVAL, *Diamond Relat. Mater.* **5** (1996) 973.
15. H. TSAI and D. B. BOGY, *J. Vac. Sci. Technol.* **5** (1987) 3287.
16. O. F. TUTTLE, *Bull. Geol. Soc. Am.* **60** (1949) 1727.
17. Y. G. GOGOTSI and M. YOSHIMURA, *MRS Bull.* **19** (1994) 39.
18. P. M. DOVE and J. D. RIMSTIDT, in "Silica", edited by P. J. Heaney, C. T. Prewitt and G. V. Gibbs (Mineralogical Society of America, Washington, DC, 1994) p. 259.
19. P. V. HUONG, *Diamond Relat. Mater.* **1** (1991) 33.
20. P. LESPADE, R. AL-JISHI and M. S. DRESSELHAUS, *Carbon* **20** (1992) 427.
21. D. S. KNIGHT and W. B. WHITE, *J. Mater. Res.* **4** (1989) 385.
22. M. YOSHIKAWA, *Mater. Sci. Forum* **52/53** (1989) 365.
23. W. WANG, T. WANG and B. CHEN, *J. Appl. Phys.* **72** (1992) 69.
24. Y. G. GOGOTSI, unpublished work (1997).
25. Y. G. GOGTSI, I.-D. JEON and M. J. McNALLAN, *J. Mater. Chem.* **7** (1997) 1841.
26. Y. G. GOGOTSI, M. J. McNALLAN, I.-D. JEON, S. WELZ, K. G.. NICKEL and T. KRAFT, *Ceram. Enging. Sci. Proc.* **19** (3/4) (1998) in press.
27. M. YOSHIMURA, J.-I. KASE, M. HAYAKAWA and S. SOMIYA, in "Corrosion and Corrosive Degradation of Ceramics", edited by R. E. Tressler and M. J. McNallan (1990) p. 337.

Received 16 December 1997
and accepted 15 May 1998